Numerical and Experimental Evaluation of Radar Absorbing Properties of Microcellular Thermoplastic Polyurethane Foam in X Band Frequency Ranges

M.H. Moeini[1], M.Hossein.N.Famili[1], K.Forooraghi[2], M.Soltani Alkouh[1], N.Ghahvechian[1]

Received:2016-05-04 Accepted:2016-07-16

Abstract

In this research, microcellular thermoplastic polyurethane foams are investigated as an absorbing material in the X-band (8.2-12.4GHz) frequency range by means of numerical analysis and experiment. In the frame of this work, we aim at establishing relationships between the foams morphology including cell size and air volume fraction and their radar absorbing properties.

We therefore first describe numerical method and modelling. Then numerical analysis of microcellular foams in various cell sizes and air volume fractions are explained. Then design basis and preparation of nanocomposite foams of various morphologies using supercritical carbon dioxide ($scCO_2$) as physical foaming agent are presented. After measuring the S-Parameters of the samples by VNA, numerical and experimental results are compared and finally we establish structure/properties relationships that are essential for further optimizations of the materials for the radar absorbing applications.

Keywords: Microcellular Foam, Radar Absorbing Properties, Thermoplastic Polyurethane, Foam Morphology, Electromagnetic Properties

1. Introduction

Due to the importance of stealth technology, Radar absorbing materials (RAM) have found special position in military projects. In recent decades, nanocomposite microcellular foams have attracted great interest due to their suitable mechanical and electromagnetic properties and controllable morphologies [1]. Attention to high stiffness, high toughness, high thermal stability, low dielectric constant, strong attenuation property at gigahertz frequency and more important of all light weight, have made them unique for the practical applications like aircrafts, missiles and warships [1-2].

The main EM wave absorption mechanism for dielectric absorbers is conductance loss which can be achieved by adding conductive fillers such as carbon black, graphite, or metal particle into polymeric matrix. In this mechanism, wave absorption material with certain electrical conductivity would produce conductance current, when an alternating electric field acted on it, and then the current would dissipate the energy in the form of heat energy [3,4]. Some researchers have used carbon black as radar absorbing additive into polymeric matrix [5-7]. However because of the strong interparticle interactions, CB[2] particles tend to form agglomerates in polymer matrices [8]. So dispersion technique is very important. The most common methods for preparing CBs composites are Melt blending, Film casting of suspensions of CBs in dissolved polymers and Co-Precipitation [7,9-12].

In many researches Co-Precipitation method has been employed [9]. Incorporating CBs into polymer raises the electrical conductivity of the insulating polymer which is necessary for EMI absorbers. This effect goes along with the increase of the relative permittivity of the material and thus reflection. Decreasing the permittivity of materials can be achieved by foaming [9-10,13-14].

There are number of researchers that have studied numerical simulation of foams. J.Zhang et al. studied absorbing properties of SiC[3] foams as novel stealthy materials by numerical simulations and theory. Finite element method and a big cube which is subtracted from nine smaller cube as a unit cell model were used for

[1]- Polymer Engineering Group, Faculty of Chemical Engineering, Tarbiat Modares University, P.O.Box:14115-111, Tehran, Iran

[2]- Communication Engineering Group, Faculty of Electrical Engineering, Tarbiat Modares University, P.O.Box:14115-111, Tehran, Iran

[2] Carbon Black

[3] Silicon Carbide

numerical analysis. They investigated dependence of coefficients of reflection on frequency at different conductivities and SiC volume fractions, for foams of 4 mm average cell diameters. To reach an understanding of the microwave absorbing mechanism, comparisons of absorbing properties among SiC-bulk, SiC-foam and SiC-particles suspended in air were conducted by means of simulation [15-16].
Numerical predictions for radar absorbing silicon carbide foams using a finite integration technique with a perfect boundary approximation are presented by H.Zhang et al. Appropriate material parameters, including the conductivity, volume fraction, cell size, thickness, and surface modified foam structure, are determined through optimization calculations, where the impedance difference between the SiC foam and free space is minimized [17].

Numerica land experimental investigation of carbon foams irradiated by EM waves, as microwave absorber, were performed by J.Zhang et al [18]. They used finite difference time domain method and tetrakaidecahedral unit-cell model for simulation and calculation of reflection coefficient of foams in different cell sizes of 2 and 3mm diameters.

Parallel variable-mesh FDTD tool for the solution of large electromagnetic problems has been research area of some researchers [28-29]. L.Catarinucci et al. proposed numerical model of metal foams and used it in a proprietary variable-mesh parallel finite difference time domain method, in order to characterize the EM properties of slabs of such materials. Also for verifying numerical results, they performed experimental evaluation of shielding effectiveness of Duocel® aluminium foam with different cell sizes and relative densities [19].
In the present work we focus our attention on the effect of morphological parameters including cell size and air volume fraction on the absorbing properties of lossy microcellular foams. In order to evaluate absorption properties of foams, computer aided design and simulation is applied and to compare with the numerical results, the absorption properties are experimentally measured by VNA in X band. In this work finite difference time domain (FDTD) method is applied to calculate the microwave absorption of the TPU[1] foams.
For the remainder the paper is organized as follows: first numerical simulation is described for lossy microcellular foams. Subsequently, material description, Foaming of TPU/CB nanocomposites in scCO2[2] and measurement technique is presented. Finally, the numerical and experimental results are discussed and compared.

2. Numerical Simulation

2.1. Theory

In electromagnetics, the behavior of EM wave can be described using partial differential equations. The field quantities electric field E and magnetic field H are related by Maxwell's equations [15]. The starting point for the construction of an FDTD algorithm is the Maxwell's time domain equation

$$\overline{\nabla} \times \vec{H} = \frac{\partial \vec{D}}{\partial t} + \vec{j} \quad (1)$$

$$\overline{\nabla} \times \vec{E} = -\frac{\partial \vec{B}}{\partial t} - \vec{M} \quad (2)$$

$$\overline{\nabla} \bullet \vec{D} = \rho_e \quad (3)$$

$$\overline{\nabla} \bullet \vec{B} = \rho_m \quad (4)$$

Where $\vec{E}$ is the electric field strength vector, $\vec{D}$ is the displacement vector, $\vec{H}$ is the magnetic field strength vector, $\vec{B}$ is the magnetic flux density vector, $\vec{j}$ is the electric current density vector, $\vec{M}$ is the magnetic current density vector, ρ_e is the electric charge density and ρ_m is the magnetic charge density.
The FDTD algorithm divides the problem geometry into a spatial grid where electric and magnetic field components are placed at certain discrete positions in space, and it solves the Maxwell's equations in time at discrete time instances. This can be implemented by first

[1] Thermoplastic Polyurethane
[2] Saturated CO_2

approximating the time and space derivatives appearing in the Maxwell's equations by finite differences and next by constructing a set of equations that calculate the values of fields at a future time instant from the values of fields at a past time instant, therefore, constructing a time marching algorithm that simulates the progression of the fields in time [26].

2.2. Model

An idealized, rectangular waveguide in X band frequency ranges (10.16×22.86 mm^2), whose schematic is shown in Fig.1, was employed in the simulation [16]. The waveguide walls are considered to be made of a perfect conductor, implying that $\hat{n}\times\overline{E}=0$ on the boundaries. This boundary condition is referred to as a PEC boundary condition. TPU foam is positioned in the middle of the waveguide. The Plane wave is excited at Port 1, and S_{11}, the voltage reflection coefficient at port 1, is calculated in order to identify the reflection of the EM wave. S_{21} is the forward voltage gain is calculated in order to identify the transmission of the EM wave [15,17].

TPU/CB foam is a dielectric foam which is consisted of two parts: nanocomposite and air cell. Real and imaginary permeability of nanocomposite is equal to one and zero, respectively. Real and imaginary permittivity of nanocomposite measured by VNA[1]. Loss tangent and dielectric constant at specific frequency are input data for the simulation. Electromagnetic parameters of air cells are as follows $\varepsilon'=1,\varepsilon''=0,\mu'=1,\mu''=0$. First order Debye model with constant loss tangent was applied for showing frequency dependence of permittivity. In order to create the foam model, initially, a cube of $10.16\times22.86\times3mm^3$ as a nanocomposite was made. Then, spheres with diameter and number according to cell size and volume fraction as air cells were subtracted from the cube in three direction coordinates. Port1 and port2 of the waveguide were located at a distance of 25mm from the center of the foam. Space between foam and ports filled with vacuum and the waveguide walls are considered to be made of a perfect conductor on the boundaries. The created model is shown in Fig. 1. This simulation was performed in the X-band frequency range (8.2–12.4 GHz), and CST Microwave Studio 2012 software package was used in the simulation. Finite difference time domain method was considered as a numerical method. In CST, meshing was automatically performed, and the mesh size was much smaller than the cell size. We used adaptive mesh refinement for proper meshing.

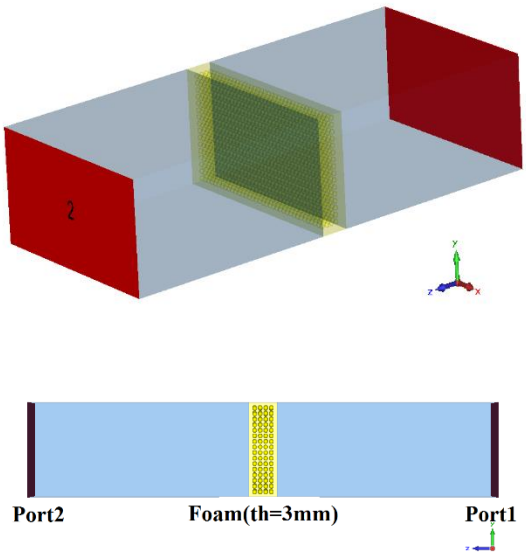

Fig. 1. Schematic of the rectangle waveguide with a TPU/C foam used in the simulation.

3. Experiments

3.1. Nanocomposite and foam preparation

Solution precipitation method used for preparation of nanocomposites which is introduced by F.Li et al [9]. Thermoplastic Polyurethane (Ravathane130A65) was first dissolved in DMF (Merck) at 60°C. TPU concentration in DMF was 0.125 gr/cc. Nano carbon black (US Nano Research, 50nm and electrical conductivity of 333 s/m) was dispersed in aceton (Merck) at concentration of $0.3mgCB/1ccAceton$ by ultrasonication for 20 minutes. Then different weight percentages of TPU solution was added into CB/aceton suspension and repeat ultrasonication for 10 more minutes. The suspension solution was poured into a surplus of distilled water. The mixture of polyurethane/CB was able to promptly precipitate from the water. The precipitated mixture was dried under vacuum. The composite samples were subsequently made

[1] Vector Network Analyzer

by compression molding at 180°C and 30 bar in a mold with the dimensions of $3\times10.16\times22.86mm^3$ in such a way that 3, 5, 10, 15, 20&25 weight percentages of CB were prepared in TPU.

To achieved various foaming characteristics, CB/TPU foams were prepared using a batch process at soaking pressures of 125 and 130 bar, soaking temperatures of 80 and 110 ºC, pressure drops of instant,1 and 3 bar/sec and stabilization times of 5 and 1000 mSec [20,30,31]. First one sample was placed into the high strength carbon steel vessel. Subsequently, CO_2 was pressurized to the soaking pressure using a booster and injected into the vessel.

The temperature is increased to the soaking temperature and the sample is kept at constant soaking temperature and pressure for 8 h to ensure the sufficient saturation's amount of CO_2 and to reach its thermodynamic solubility.

After the soaking time, a rapid depressurization was applied then after short period of time which is called stabilization time, pressurized cold fluid ($-12^{\circ C}$) was injected into the vessel in order to stabilize the foams. Sample with 15wt% of CB was used for foaming. Overall, process condition for foaming of TPU with 15wt% of CB is shown in table 1.

Foaming process condition setting and modelling were accomplished in such a way that volume fraction and cell size of foam in both numerical evaluation and experimental evaluation would be nearest to each other.

Table. 1. Foaming process condition of 15wt% of CB nanocomposi

Sample NO.	Temperature (˚C)	Pressure (bar)	Stabilization Time	$\frac{dP}{dt}$ $(\frac{bar}{s})$	Volume fraction of air
A1	110	125	5ms	instantly	0.78
A2	110	125	1s	3	0.8
A3	110	125	1s	1	0.79
B1	80	130	5ms	instantly	0.41
B2	80	130	1s	3	0.41
B3	80	130	1s	1	0.42

3.2.Measurement

3.2.1. Electromagnetic properties measurement

The measurements were performed using a vector network analyzer (VNA) Model E8362B (Agilent) in X-band frequency range. Dimensions of un-foamed samples were exactly fit to WR90 waveguide but foamed samples were cut by die cut mold shown in Fig. 2.

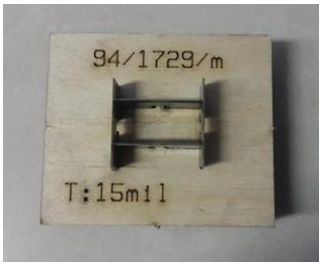

Fig. 2. Schematic of the die cut mold $(10.16\times22.86mm^2)$.

Then sample was positioned into the fixture between the flanges of waveguide. Finally the S-parameters are measured. Schematic of the VNA is shown in Fig. 3.

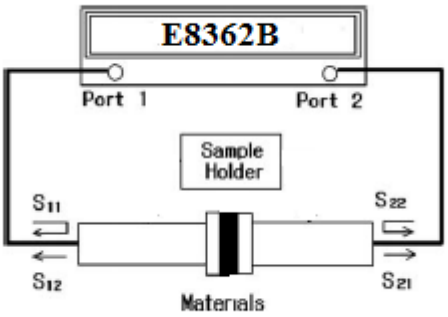

Fig. 3. Test setup for radar absorbing efficiency measurement.

Amplitude and phase of S-parameters were produced by VNA. Extraction of both

permittivity and permeability $(\varepsilon', \varepsilon'', \mu', \mu'')$ from S-parameters was performed using the Nicolson-Ross-Weir algorithm. Magnitude of S-parameters were calculated by $(10^{\frac{amplitude}{20}})$ and finally according to the following equations reflection, transmission and absorption were calculated [21].

$$reflection\,(\%) = |S_{11}|^2 (= |S_{22}|^2) \times 100 \quad (5)$$

$$transmission(\%) = |S_{21}|^2 (= |S_{12}|^2) \times 100 \quad (6)$$

$$absorption(\%) = 100 - reflection\,(\%) - transmission(\%) \quad (7)$$

Conductivity and electrical loss tangent were determined by the following equations [22].

$$\sigma = \omega \varepsilon_0 \varepsilon'' \quad (8)$$

$$\tan\delta_e = \frac{\varepsilon''}{\varepsilon'} \quad (9)$$

Where $\sigma, \omega, \varepsilon'', \varepsilon', \tan\delta_e$ are respectively electrical conductivity $(\frac{s}{m})$, angular frequency, imaginary permittivity, real permittivity and electrical loss tangent.

3.2.2. Cell size measurement

The microstructures of the foams were observed with a Philips XL30 scanning electron microscope (SEM). The samples were freeze-fractured after immersion in liquid nitrogen for 20 min and the fractured surfaces were coated with a thin layer of platinum before the SEM observation. Cell size was measured by "MEASUREMENT" software. SEM micrographs were imported into the software, after calibrating software ruler, cell sizes were determined.

3.2.3. Density

Foam density is measured according to ASTMD792 then volume fraction of air was calculated by following equation.

$$v_{air} = 1 - \frac{\rho_{Foam}}{\rho_{Polymer}} \quad (10)$$

4. Results and discussion

Figure. 4 shows average variation of conductivity of TPU nanocomposite in the X-band frequency range. It is evident that conductivity is affected by the weight percentage of nanocarbon black. Conduction can be observed to remain negligible at very small nanocarbon black content, which does not allow the formation of conducting channels. The percolation threshold is found at 15 wt% where the electrical conductivity of the composite jumps up. This behavior is attributed to the formation of conducting network through the matrix [7]. The curve drop at 25% which is attributed to the agglomeration of nanoparticles at highly loaded polymers. When nanoparticles get agglomerated, poor conducting network is formed.

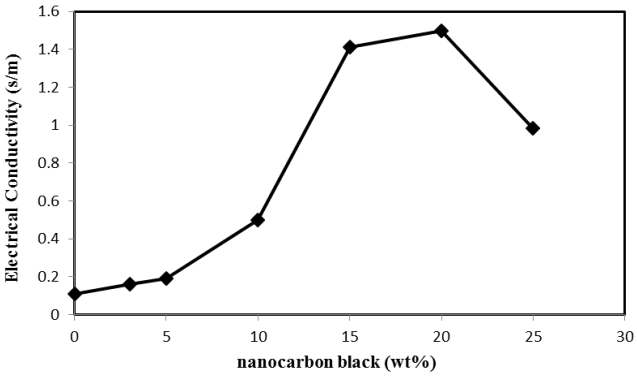

Fig. 4. Electrical conductivity of the CB/TPU nanocomposite versus the CB weight percentage.

The 15 wt% nanocomposite was used for foaming because it was above percolation threshold so it's electrical conductivity and loss tangent was considerable. Figure. 5 shows frequency dependency of real and imaginary permittivity of the 15 wt% nanocomposite which is derived from the first order Debye model with constant loss tangent and experiment. As seen from Fig. 5 Debye model is a good fit to the experimental results.

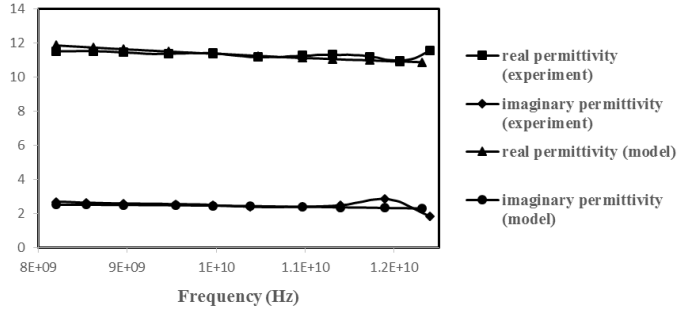

Fig. 5. Real and imaginary permittivity of 15 wt% CB/TPU nanocomposite which is derived from the first order Debye model and experiment.

Figure. 6 shows a representative SEM micrograph of the cross section of the carbon

black-TPU nanocomposite foam with 15 wt% nanocarbon black. It is evident that the microcellular cells were distributed throughout the foam. These nearly spherical cells exhibit an average cell size from 2 to 10 μm in diameter which could be seen in table 2. The formation of this unique microcellular structure and homogenous cell size is attributed to the use of supercritical CO_2 as the foaming agent [30,31].

The TPU foam can be fabricated with different cell sizes and volume fractions, which can be obtained in the model and experiment by changing the diameter and the number of air cells. The numerical and experimental investigation of the effects of the volume fraction and cell size of TPU foam on the electromagnetic properties in the X-band frequency range are presented in this section.

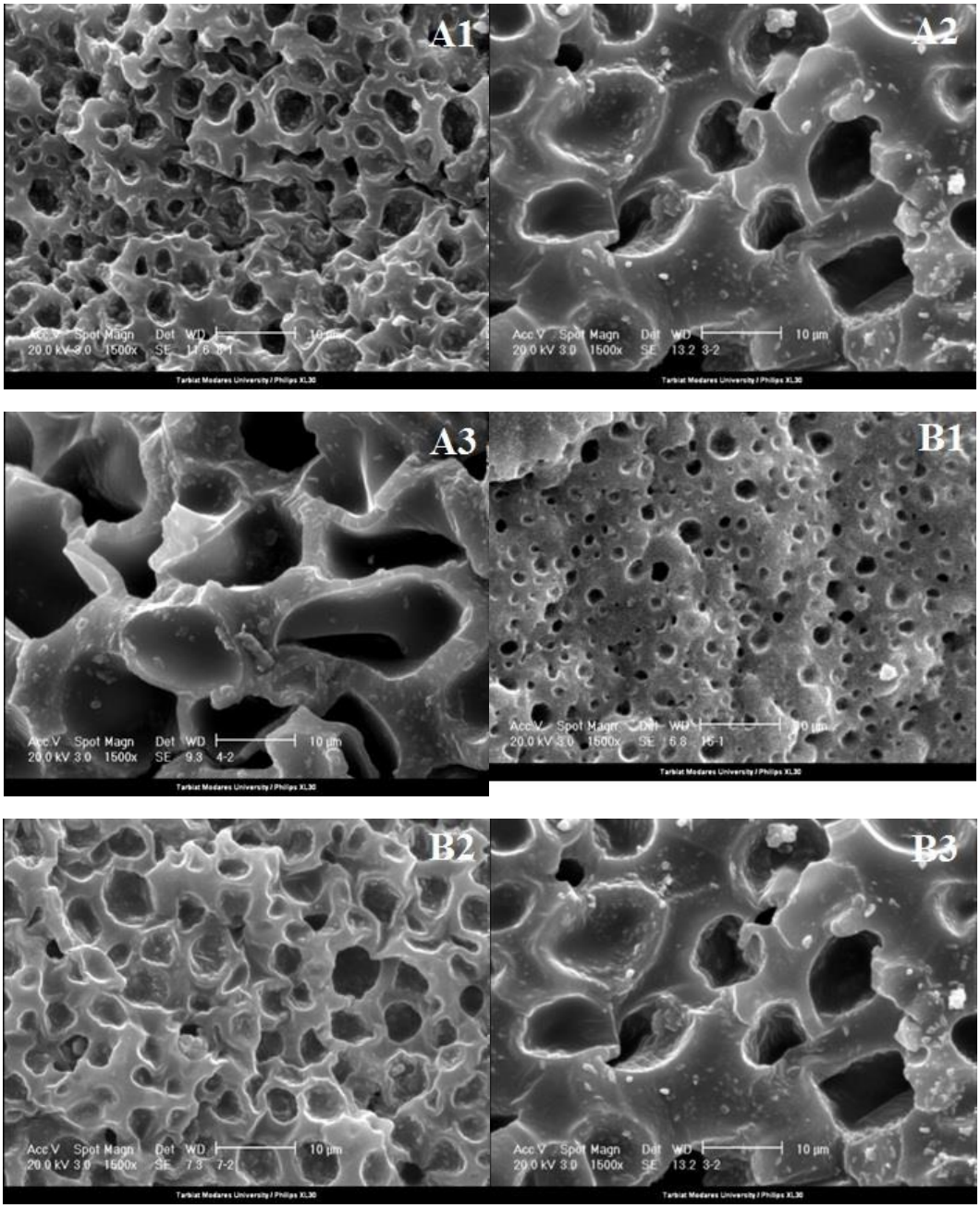

Fig. 6. SEM images of the cross-section of TPU nanocomposite microcellular foam with 15 wt % carbon black for A_1,A_2,A_3,B_1,B_2&B_3 samples.

Table. 2. Cell size and air volume fraction for different samples

Sample NO.	Average cell size (μm)	Standard deviation	Volume fraction of air
A1	2	0.82	0.78
A2	5	0.85	0.8
A3	10	0.78	0.79
B_1	2	0.39	0.41
B2	5	0.45	0.41
B3	10	0.34	0.42

Fig. 7. Electromagnetic properties of 15 wt% nanocomposite vs frequency

4.1. The effect of volume fractions of air on absorbability

The numerical and experimental investigation of the effect of the air volume fractions at fixed cell size 10 µm on absorbability of foam is presented in this section.
properties of 15 wt% CB/TPU nanocomposite was measured by VNA as is shown in Fig. 7.

4.1.1. Numerical evaluation

Electromagnetic properties of air was considered equal to vacuum ($\varepsilon' = 1, \varepsilon'' = 0, \mu' = 1, \mu'' = 0$) and electromagnetic

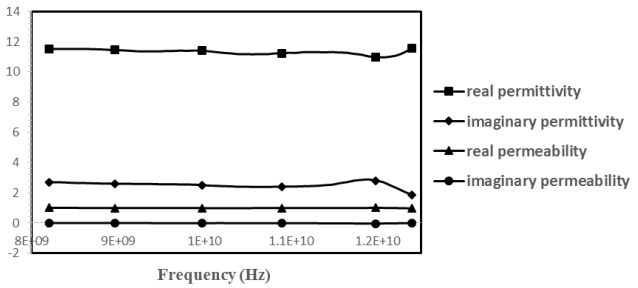

Fig. 7. Electromagnetic properties of 15 wt%

nanocomposite vs frequency Foam thickness of 3 mm and air cell diameter of 10 µm is used. The fractions of air in TPU foam were 0.79 and 0.46. S-parameters were determined by finite difference time domain method in X band frequency range, and then percentage of reflection, transmission and absorption calculated by equations 5-7.
As seen from figure. 8(a), the reflection is affected by the air volume fraction at fixed cell size where it is reduced with an increase in air volume fraction. This is due to the high effective permittivity of the foam with low volume fraction and therefore the impedance of the foam mismatches with free space too much. Consequently, most of the wave is reflected from the surface of the foam and is not absorbed. Dispersing conductive filler into the insulating matrix raises the electrical conductivity of the matrix and this effect goes along with the increase of the relative permittivity of the material promoting EM wave reflections, which is undesirable for RAMs. Decreasing the permittivity of materials can be achieved by foaming [27,31].
As shown in Fig. 8(b) Transmission is a function of air volume fraction and is reduced with an increase in air volume fraction. Since air cells are small with respect to wavelength, Effective Medium Theory (EMT) is used to estimate average permittivity and permeability of the inhomogeneous material. There are number of formulas for calculating the effective medium, among which the Maxwell–Garnett (M–G) theory and the Bruggeman (Br) theory are widely used. So according to Effective Medium Theory, the microcellular foam could be assumed as an effective medium which its permittivity is reduced with an increase in air volume fraction. Therefore the impedance of the foam matches with free space and the transmission is increased [16,25].
Wave absorption ability of un-foamed nanocomposite is higher than foamed nanocomposite as is observed from Fig. 8(c). The lower the air volume fraction, the higher the absorption ability. Electromagnetic loss in bulk material is the main phenomena which causes power absorption. Foaming is a cause of an electrical loss tangent and therefore absorption

reduces at the same thickness. Foaming reduces the bulk density, so mass of material reduces at the same thickness. Considering that absorption is related to the mass of lossy medium, therefore, correct comparison is comparison of absorption per weight of foamed and un-foamed samples. As shown in Fig. 9 Minimum Absorption (%) per weight is attributed to un-foamed sample and with an increase in air volume fraction, Absorption (%) per weight increases. The cause of this phenomenon can be attributed to the fact that foaming makes multiple scattering inside the porous material and finally electromagnetic waves are attenuated.

Therefore, foaming causes the reduction of permittivity and reflection and also an increase of absorption per weight, resulting in an improvement of radar absorbing properties.

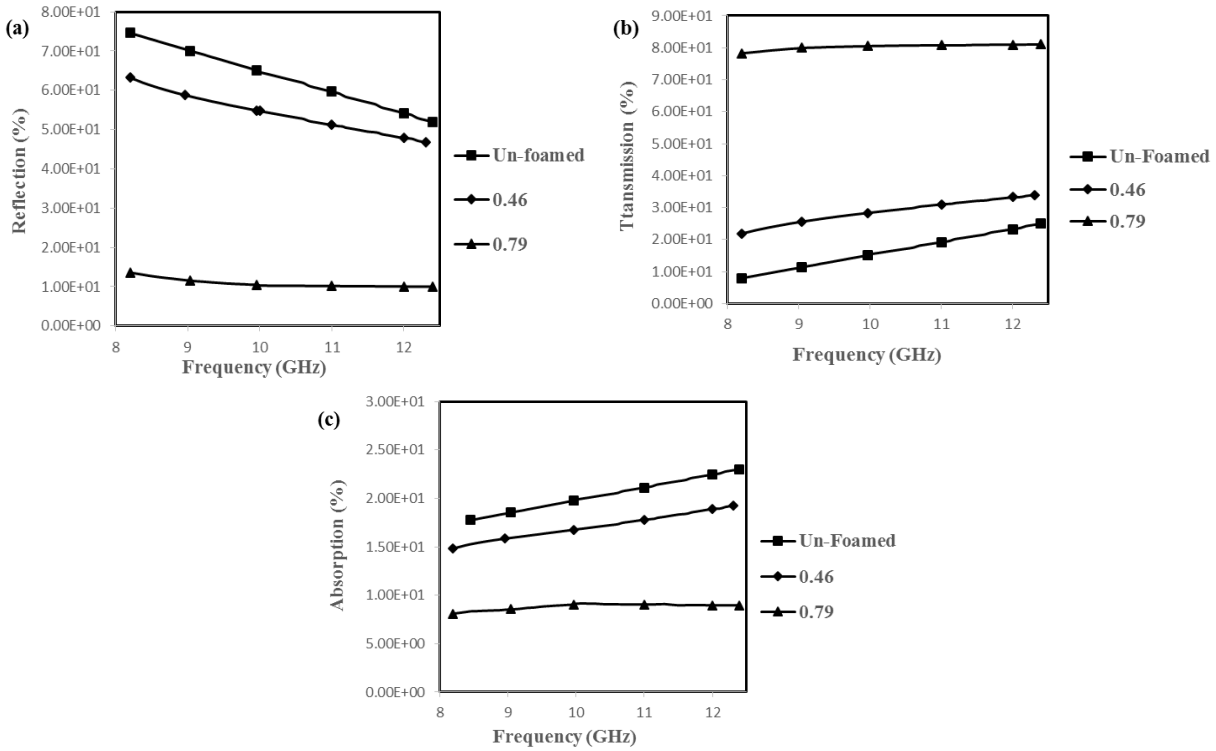

Fig. 8. Variations of (a) reflection (%), (b) transmission (%) and (c) Absorption (%) vs frequency of un-foamed nanocomposite (TPU-15%CB) and foams at fixed cell size 10μm and different air volume fractions (0.46 , 0.79).

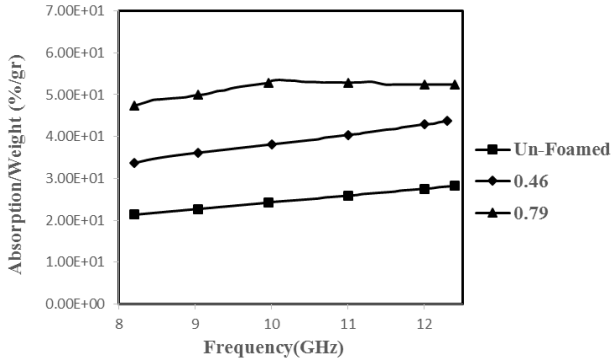

Fig. 9. Variations of absorption per weight vs frequency of un-foamed nanocomposite (TPU-15% CB) and foams at fixed cell size of 10μm and different volume fractions of air (0.46 , 0.79).

4.1.2. Experimental evaluation

The effect of volume fractions of air at fixed cell size on absorbability of foam, is investigated in this section. Samples A_3 and B_3 were compared. Samples with dimensions of $3\times10.16\times22.86$ mm^3 were prepared. S-Parameters were obtained from VNA and using equations 5-7, reflection, transmission and absorption were calculated.
Variations of reflection, transmission and absorption of nanocomposite and foam shown in Fig. 10.

Similar to numerical results, maximum reflection is ascribed to the un-foamed sample. Reflection is reduced with an increase in air volume fraction. Minimum transmission is attributed to the un-foamed sample. Transmission is increased with an increase in air volume fraction. Un-foamed nanocomposite showed greater absorption in comparison with foamed nanocomposites at the same thickness.

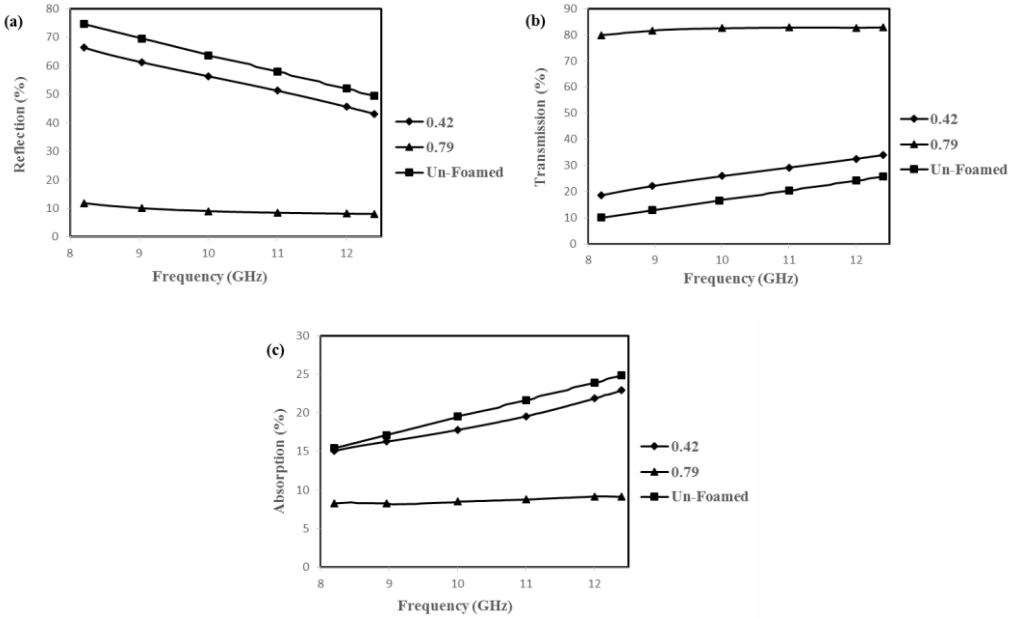

Fig. 10. Variations of (a) reflection (%), (b) transmission (%) and (c) absorption (%) vs frequency of the un-foamed nanocomposite (TPU-15%CB) and foams at fixed cell size of 10μm and different air volume fractions (0.42 , 0.79)

Considering that foaming reduces density of sample, absorption (%) per weight is a correct criterion for evaluation of absorbing foam or nanocomposite. As seen from Fig. 11 similar to numerical results minimum absorption (%) per weight is attributed to the un-foamed sample and is increased with an increase in air volume fraction which could be attributed to the multiple scattering inside the porous material and so EM wave loss.

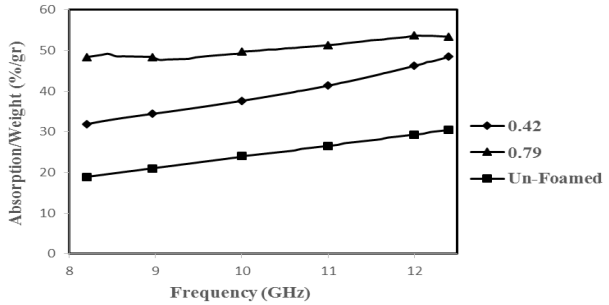

Fig. 11. Variations of absorption (%) per weight vs frequency of un-foamed nanocomposite (TPU-15%CB) and the foams at fixed cell size $(10\mu m)$ and different air volume fractions (0.46 , 0.79).

4.2. The effect of cell size on absorbability

Numerical and experimental investigation of the effect of cell size at fixed volume fraction (0.4) on absorbability of foam is presented in this section.

4.2.1. Numerical evaluation

Electromagnetic properties of air was considered equal to vacuum and also electromagnetic properties of 15 wt% CB/TPU nanocomposite was shown in Fig. 7**.** The foams were 3mm in thickness and 5µm, 10µm, 1mm and 2mm in cell diameters. S-parameters were determined by finite difference time domain method in X band frequency range, and then percentage of reflection, transmission and absorption were calculated by equations 5-7. Variations of reflection, transmission and absorption of foams for different cell sizes at two volume fractions (0.39, 0.4) are shown in Fig. 12.

As shown in Fig. 12(a), reflection is a little affected by the cell size and is increased with a decrease in cell size. Reflections of samples with cell size of 5 and 10µm and also 1 and 2mm are near to each other. When the foam cell size is reduced at fixed air volume fraction, the number of cells is increased and therefore scattering is increased. Transmission is reduced with the reduction of cell size as is observed from Fig. 12(b). Absorption is also affected by cell size as shown in Fig. 12(c). The lower the cell size, the higher the absorption. This is attributed to the greater number of cells in the foam create more multiple scattering inside the material which can be serious mechanism for EM wave attenuation as shown in Fig. 13.

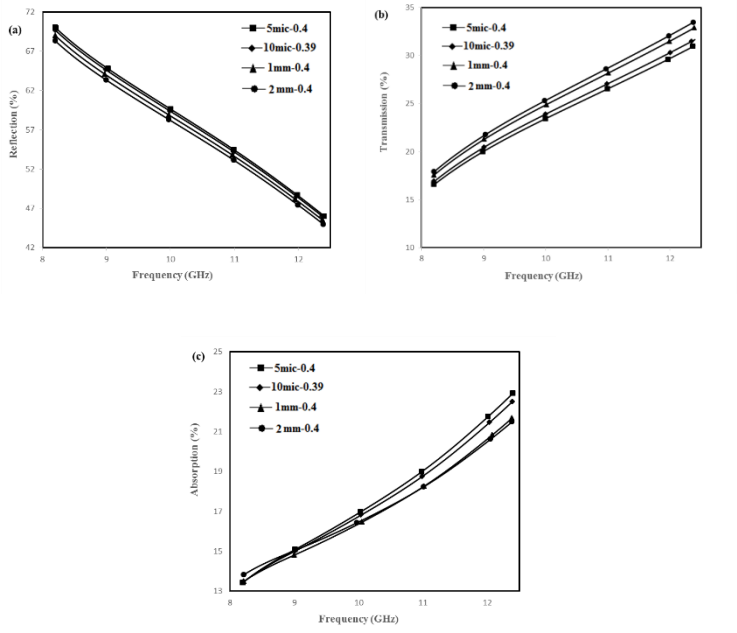

Fig. 12. Variations of (a) reflection (%), (b) transmission (%) and (c) absorption (%) vs frequency of the foams at two air volume fractions $(0.39 \& 0.4)$ and different cell sizes (5µm, 10µm, 1mm and 2mm cell diameters).

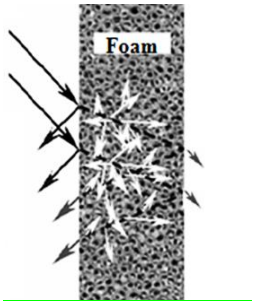

Fig. 13. Schematic of multiple scattering inside the nanocomposite foams caused by reducing the cell size.

Comparing the results shown in figures 8 and 12, it is obvious that reflection, transmission and absorption are more affected by air volume fraction than the cell size. This indicates that for the foams considered, since the foam cell size is much smaller than the incident wavelength in X band frequency range; the long wavelength radiation is too myopic to detect the foam size or insensitive to the foam structure [17]. But when various foam cell sizes show the various reflection, transmission and absorption even a little, it means that behavior of the foam against EM wave deviates a little from EMTs. Because in EMTs, electromagnetic properties of medium are only affected by volume fraction of inclusions not size of inclusions [25].

4.2.2. Experimental evaluation

The effect of cell size at fixed volume fraction of air on absorbability of the foam, is investigated in this section. Samples B_1, B_2 and B_3 were compared. Samples with dimension of $3\times10.16\times22.86$ mm^3 were prepared. S-Parameters were obtained from VNA and employing equations 5-7, reflection, transmission and absorption were calculated. Variations of reflection, transmission and absorption of the foams are shown in figure. 14. Similar to numerical results reflection is a little affected by the cell size and is increased with a decrease in cell size as shown in Fig. 14(a). Transmission is reduced with a reduction of cell size as is observed from Fig. 14(b). Absorption is also a little affected by the cell size as seen from Fig. 14(c). The lower the cell size, the higher the absorption.

4.3. Comparison of numerical and experimental results

Numerical and experimental results for different cell sizes and volume fractions is compared in this section.

4.3.1. Variations of volume fractions at fixed cell size

Comparison of numerical and experimental results for reflection, transmission and absorption is shown in Fig. 15,16. As is seen from figures experimental results completely verify the numerical results.

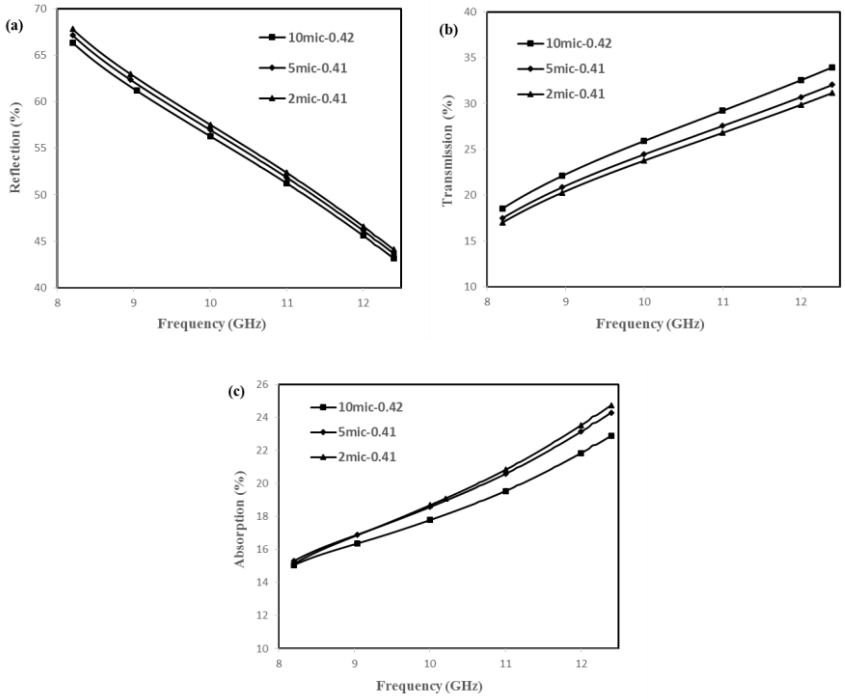

Fig. 14 Variations of (a) reflection (%), (b) transmission (%) and absorption (%) vs frequency of the foams at two air volume fractions (0.41,0.42) and different cell sizes (2μm, 5μm and 10μm in diameter).

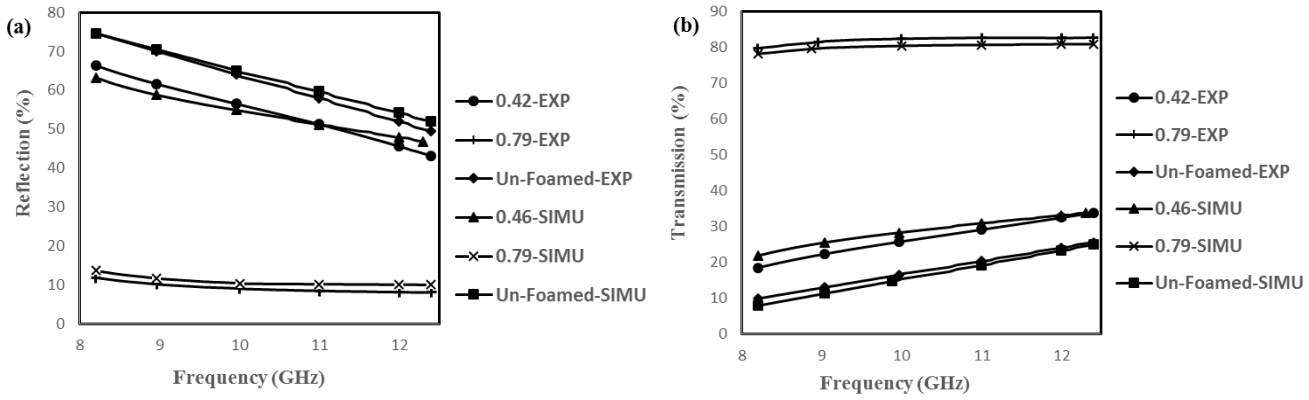

Fig. 15. Numerical and experimental results for (a) reflection (%) and (b) transmission (%) of the un-foamed nanocomposite (15%CB-TPU) and the foams vs frequency at fixed cell size (10μm) and different volume fractions.

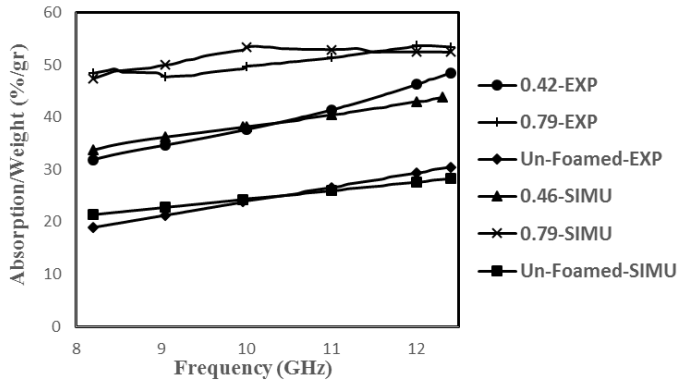

Fig. 16. Numerical and experimental results for absorption of the un-foamed nanocomposite and the foams vs frequency at fixed cell size (10μm) and different volume fractions.

4.3.2. Variations of foam cell sizes at fixed volume fraction

Comparison of numerical and experimental results for reflection, transmission and absorption is shown in Fig. 17.

Trend of reflection in the experimental results is similar to the numerical results but quantities in numerical is a little higher than experimental as seen in Fig. 17(a). This is attributed to the lower volume fraction in numerical analysis. In fact, preparation of sample which it's air volume fraction would be exactly the same as the model in numerical analysis or vice versa preparation of model which it's air volume fraction would be exactly the same as the sample in experimental analysis, is not possible. Also this is true for transmission and absorption. From experimental results it is found that absorption of the foam for the different cell sizes is more affected in comparison to the numerical results. This is attributed to numerical method. In fact finite difference time domain method is insensitive to variation of foam cell size from 5μm to 10μm.

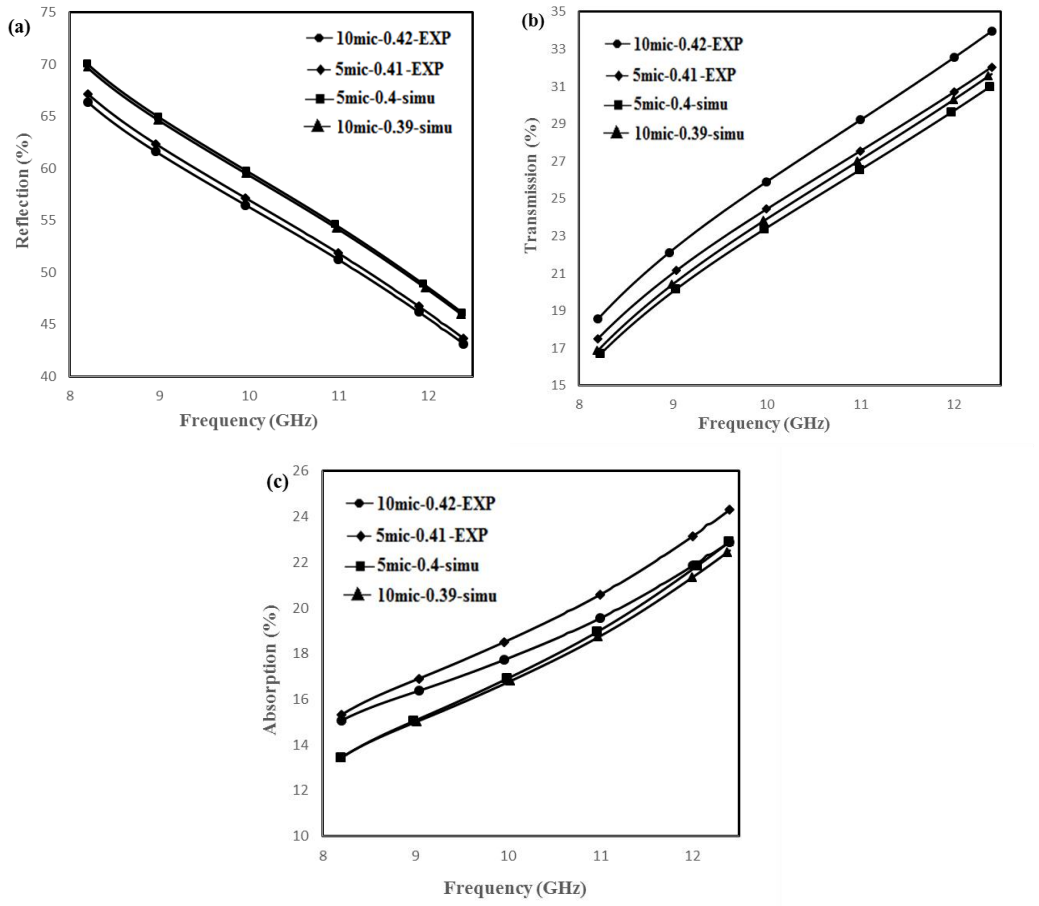

Fig. 17. Numerical and experimental results for (a) reflection (%), (b) transmission (%) and (c) absorption (%) of the foams vs frequency at approximately fixed volume fraction and different cell sizes.

5. Conclusion

In this paper, microcellular thermoplastic polyurethane foams with various cell sizes and air volume fractions were prepared as absorbing materials and electromagnetic properties of the foams by means of experimental and numerical analysis in the X-band frequency range were investigated. The following conclusions are drawn from this study:

1. The foaming caused a strong reduction in dielectric constant and reflection.
2. An increase in air volume fraction at fixed foam cell size makes absorption per weight of the foam increase, which is due to multiple scattering inside the porous materials.
3. Reducing the foam cell size at fixed air volume fraction makes percentage of absorption increase. It means that microcellular foams shows a little deviation from EMTs. Therefore microcellular foams as radar absorbing materials have special importance.
4. Sensitivity of electromagnetic wave against the variations of cell size is strongly lower than variations of air volume fraction because the cell size is much smaller than the incident wavelength.
5. The combination of these two concepts, microcellular foams and carbon filler, are very promising for the design of materials for light radar absorbing applications. Indeed, the dispersion of CBs in a polymer matrix imparts it the required electrical conductivity that is essential for the interaction of the material with the electromagnetic radiation. The foaming of the nanocomposite ensures the preservation of a low dielectric constant that limits the reflection of EM radiation at the material interface.
6. Finite Difference Time Domain method is a suitable method for evaluation of microcellular foams and it's conformity with experimental results is acceptable.
7.

References

[1] Minh-Phuong Tran, Christophe Detrembleur, Michaël Alexandre, Christine Jerome and Jean-Michel Thomassin, "***The influence of foam morphology of multi-walled carbon nanotubes/poly(methyl methacrylate) nanocomposites on electrical conductivity***", Polymer, 54, 2013, 3261-3270.

[2] Hao-Bin Zhang, Qing Yan, Wen-Ge Zheng, Zhixian He and Zhong-Zhen Yu, "***Tough Graphene-Polymer Microcellular Foams for Electromagnetic Interference Shielding",*** Applied materials & interfaces, 3, 2011, 918-924.

[3] Ki-Yeon Park, Sang-Eui Lee, Chun-Gon Kim and Jae-Hung Han, "***Fabrication and electromagnetic characteristics of electromagnetic wave absorbing sandwich structures",*** Composites Science and Technology, 66, 2006, 576-584.

[4] Jia Huo, Li Wang and Haojie Yu, "***Polymeric nanocomposites for electromagnetic wave absorption"***, Materials Science, 44, 2009, 3917-3927.

[5] Woo-Kyun Jung, Beomkeun Kim, Myung-Shik Won and Sung-Hoon Ahn, "***Fabrication of radar absorbing structure (RAS) using GFR-nano composite and spring-back compensation of hybrid composite RAS shells"***, Composite Structures, 75, 2006, 571-576.

[6] Jung-Hoon Oh, Kyung-Sub Oh, Chun-Gon Kim and Chang-Sun Hong, "***Design of radar absorbing structures using glass/epoxy composite containing carbon black in X-band frequency ranges"***, Composites: Part B, 35,2004, 49-56.

[7] T. Gurunathan, Chepuri R. K. Rao, Ramanuj Narayan and K. V. S. N. Raju, "***Polyurethane conductive blends and composites: synthesis and applications perspective"***, Materials Science, 48, 2013, 67-80.

[8] Mao Peng, Mingxing Zhou, Zhijiang Jin, Weiwei Kong, Zhongbin Xu and Damien Vadillo, ***"Effect of surface modifications of carbon black (CB) on the properties of CB/polyurethane foams"***, Materials Science, 45, 2010, 1065-1073.

[9] Fengkui li, Lanying qi, Jiping yang, Mao xu, Xiaolie luo and Dezhu ma, "***Polyurethane/Conducting Carbon Black Composites: Structure, Electric Conductivity, Strain Recovery Behavior, and Their Relationships***", Applied Polymer Science, 75, 2000, 68-77.

[10] Chuanxi Xiong, Zhiyong Zhou, Wei Xu, Huirong Hu, Yi Zhang and Lijie Dong**,** ***"Polyurethane/carbon black composites with high positive temperature coefficient and low critical transformation temperature"***, Carbon, 43, 2005, 1778-1814.

[11] Ivan Chodak, Maria Omastova and Jurgen Pionteck, ***"Relation Between Electrical and Mechanical Properties of Conducting Polymer Composites",*** Applied Polymer Science, 82, 2001, 1903-1906.

[12] I.Novak, I.Krupa, I.Chodak, ***"Relation between electrical and mechanical properties in polyurethane/carbon black adhesives"***, Materials Science Letters, 21, 2002, 1039-1041.

[13] Nicolas Quievy, Pierre Bollen, Jean-Michel Thomassin, Christophe Detrembleur, Thomas Pardoen, Christian Bailly and Isabelle Huynen, ***"Electromagnetic Absorption Properties of Carbon Nanotube Nanocomposite Foam Filling Honeycomb Waveguide Structures"***, IEEE Transactions on Electromagnetic Compatibility, 54, 2012, 43-51.

[14] Jean-Michel Thomassin, Christophe Pagnoulle, Lukasz Bednarz, Isabelle Huynen, Robert Jerome and Christophe Detrembleur, ***"Foams of polycaprolactone/MWNT nanocomposites for efficient EMI reduction"***, Materials Chemistry, 18, 2008, 792-796.

[15] Hongtao Zhang, Jinsong Zhang and Hongyan Zhang, "***Computation of radar absorbing silicon carbide foams and their silica matrix composites"***, Computational Materials Science, 38, 2007, 857-864.

[16] Hongtao Zhang, Jinsong Zhang, Hongyan Zhang, ***"Electromagnetic properties of silicon carbide foams and their composites with silicon dioxide as matrix in X-band"***, Composites Part A, 38, 2007, 602-608.

[17] Hongtao Zhang, Jinsong Zhang and Hongyan Zhang, "***Numerical predictions for radar absorbing silicon carbide foams using a finite integration technique with a perfect boundary approximation***", Smart Materials and Structures, 15, 2006, 759-766.

[18] Zhigang Fang, Xiaoming Cao, Chusen Li, Hongtao Zhang, Jinsong Zhang, Hongyan Zhang, ***"Investigation of carbon foams as microwave absorber: Numerical prediction and experimental validation"***, Carbon, 44, 2006,

[19] L. Catarinucci, G. Monti and L. Tarricone, ***"metal foams for electromagnetics: experimental, numerical and analytical characterization"***, Progress in Electromagnetics Research, 45, 2012, 1-18.

[20] M.mokhtari Motameni shirvan, M.H.N. Famili, M.Soltani Alkouh, A.Golbang, "***The Effect of pressurized and fast stabilization on one step batch foaming process for the investigation of cell structure formation***," Supercritical Fluids, 112, 2016, 143-152.

[21] Y. K. Hong, C. Y. Lee, C. K. Jeong, D. E. Lee, K. Kim, ***"Method and apparatus to measure electromagnetic interference shielding efficiency and its shielding characteristics in broadband frequency ranges"***, Review of Scientific Instruments, 74, 2003, 1098-1102.

[22] Ting Zhanga, Daqing Huangb, Ying Yangd, Feiyu Kanga and Jialin Gub, ***"Fe3O4/carbon composite nanofiber absorber with enhanced microwave absorption performance"***, Materials Science and Engineering B, 178, 2013, 1-9.

[23] M. Soltani Alkuh, M.H.N. Famili, M.Mokhtari Motameni Shirvan, M.H.Moeini, "***The relationship between electromagnetic absorption properties and cell structure of poly(methyl methacrylate)/multi-walled carbon nanotube,***" Materials and Design, 100, 2016, 73-83.

[24] Yu-Qing Kang, Mao-Sheng Cao, Jie Yuan, Lu Zhang, Bo Wen and Xiao-Yong Fang, ***"Preparation and microwave absorption properties of basalt fiber/nickel core–shell heterostructures"***, Alloys and Compounds, 495, 2010, 254-259.

[25] Ludmilla Kolokolova and Bo A.S. Gustafson, ***"Scattering by inhomogeneous particles: microwave analog experiments and comparison to effective medium theories"***, Quantitative Spectroscopy & Radiative Transfer, 70, 2001, 611-625.

[26] Altef Z.Elsherbeni and Veysel Demir, "***The Finite-Difference Time-Domain Method for Electromagnetics With MATLAB Simulations***," Scitech, USA, 2009, pp.1-10.

[27] Constantine A.Balanis, ***"Advanced Engineering Electromagnetics"***, John Wiley & Sons, USA, 1989, 180-229.

[28] L. Catarinucci, P. Palazzari, L.Tarricone, ***"A Parallel Variable-Mesh FDTD Algorithm for the Solution of Large Electromagnetic Problems"***, Proceedings of the 19th IEEE International Parallel and Distributed Processing Symposium (IPDPS'05)

[29] Luca Catarinucci, Paolo Palazzari and Luciano Tarricone, ***"A Parallel FDTD Tool for the Solution of Large Dosimetric Problems: an Application to the Interaction between Humans and Radio b,ase Antennas"***, Microwave Symposium Digest, 2002 IEEE MTT-S International.

[30] Maziar Soltani Alkouh, M. Hossein N. Famili and M. Hasan Moeini, ***"The investigation of Foaming Effect on Radar Absorbing Properties of PMMA/MWCNT Composites"***, Iranian Journal of Polymer Science and Technology, 28, 2015, 189-195.

[31] M. Mokhtari Motameni Shirvan and M. H. N. Famili, "***Effect of stabilization on the morphology of polystyrene and scCO2 foam***", Iran. J. Polym. Sci. Technol. (Persian), 28, 2015, 505-515.